

Advances in Theory and Simulations of Large-Scale Dynamos

Axel Brandenburg

Received: 7 September 2008 / Accepted: 25 January 2009 / Published online: 21 February 2009
© Springer Science+Business Media B.V. 2009

Abstract Recent analytical and computational advances in the theory of large-scale dynamos are reviewed. The importance of the magnetic helicity constraint is apparent even without invoking mean-field theory. The tau approximation yields expressions that show how the magnetic helicity gets incorporated into mean-field theory. The test-field method allows an accurate numerical determination of turbulent transport coefficients in linear and nonlinear regimes. Finally, some critical views on the solar dynamo are being offered and targets for future research are highlighted.

Keywords Solar dynamo · Sun · Magnetic fields · Magnetic activity

1 Introduction

Over the past 50 years significant progress has been made in understanding the origin of the solar magnetic field. In an important paper, Parker (1955) introduced the idea of mean magnetic fields and identified the α effect as the crucial ingredient of large-scale dynamos. He also proposed and solved an explicit one-dimensional mean-field model and found the migratory Parker dynamo wave. This provided an important tool for understanding the effects of α and shear, and it led to useful estimates for the excitation conditions, the cycle period, and the direction of field migration in solar and stellar dynamo models. However, Parker's work appeared at a time when it was still unclear whether homogeneous fluid dynamos really exist. These are dynamos of uniformly conducting matter, without insulating wires that are thus susceptible to "short circuits". In the years following Cowling's (1933) theorem, it remained doubtful whether the Sun's magnetic field can be explained in terms of dynamo theory, as originally anticipated by Larmor (1919).

In the paper on his famous theorem, Cowling (1933) concluded "The theory proposed by Sir Joseph Larmor, that the magnetic field of a sunspot is maintained by the currents it induces in moving matter, is examined and shown to be faulty; the same result also applies

A. Brandenburg (✉)
Nordita, Roslagstullsbacken 23, 10691 Stockholm, Sweden
e-mail: brandenb@nordita.org

for the similar theory of the maintenance of the general field of Earth and Sun.” Larmor (1934) responded that “the self-exciting dynamo analogy is still, so far as I know, the only foundation on which a gaseous body such as the Sun could possess a magnetic field: so that if it is demolished there could be no explanation of the Sun’s magnetic field even remotely in sight.”

Although the first qualitative ideas on homogeneous dynamos were proposed nearly a hundred years ago, the resistance was immense; for historical accounts see the reviews by Krause (1993) and Weiss (2005). An important existence proof for homogeneous self-excited dynamos was that of Herzenberg (1958), who showed, using asymptotic theory, that dynamos work in a conducting medium where two rotors spin about axes that lie in planes perpendicular to their direction of separation, and inclined relative to each other by an angle between 90° and 180° . Such systems were later realized experimentally by Lowes and Wilkinson (1963, 1968). In their experiments oscillations commonly occurred. Those were thought to be some kind of nonlinear relaxation oscillations. However, they used angles of less than 90° . Indeed, when the relative angle between the rotors is between 0° and 90° , oscillatory solutions are expected even from linear theory (Brandenburg et al. 1998). Those solutions were not captured by the original analysis of Herzenberg (1958), because he only looked for steady solutions.

The next important steps came with the development of mean-field electrodynamics by Steenbeck et al. (1966), who used the first order smoothing approximation (or second order correlation approximation) as a rigorous tool to compute α effect and turbulent diffusivity in limiting cases. Steenbeck and Krause (1969) later produced global mean-field models in spherical geometry and computed synthetic butterfly diagrams. For an introduction to mean-field theory we refer to the article by N.O. Weiss in this issue.

The technical tools made available by mean-field theory have stimulated much of the research in the field during the 1970s. However, during the 1980s a number of problems were discussed. For example, doubts were raised whether turbulent magnetic diffusion still works at large magnetic Reynolds numbers, R_m ; see work by Knobloch (1978), Layzer et al. (1979) and Piddington (1981). This problem applies equally to kinematic and nonlinear cases. Regarding the kinematic α effect, Childress (1979) found that in steady convection α decreases with increasing R_m like $R_m^{-1/2}$. This result is now understood to be a common feature of steady flows (Rädler et al. 2002; Rädler and Brandenburg 2009), and is generally not shared by unsteady (e.g. turbulent) flows (Sur et al. 2008).

The nonlinear problem was a focus of much of the work on dynamos during the 1990s, and started with the work of Cattaneo and Vainshtein (1991, hereafter referred to as CV91) who showed, using two-dimensional turbulence simulations, that for $\overline{\mathbf{B}}^2 \approx B_{\text{eq}}^2$, η_t decreases like R_m^{-1} . It was expected that a similar relation applies also to α (Vainshtein and Cattaneo 1992, hereafter VC99), but this required three-dimensional considerations. Indeed, using uniform imposed fields, Cattaneo and Hughes (1996, hereafter CH96) showed that α decays with increasing R_m like R_m^{-1} . These results were later understood to be due to the presence of conservation laws for the mean squared vector potential, $\langle \mathbf{A}^2 \rangle$, in two dimensions and the magnetic helicity, $\langle \mathbf{A} \cdot \mathbf{B} \rangle$, in three dimensions Gruzinov and Diamond (1994, hereafter GD94, 1995). Here, \mathbf{A} is the magnetic vector potential with $\mathbf{B} = \nabla \times \mathbf{A}$. However, these conservation laws only tell us how much small-scale magnetic field is being produced as the mean-field dynamo produces large-scale field, such that $\langle \mathbf{A}^2 \rangle$ (in two dimensions) or $\langle \mathbf{A} \cdot \mathbf{B} \rangle$ (in three dimensions) remain unchanged. One still needs a theory that relates the corresponding small-scale mean squared vector potential to the turbulent magnetic diffusion in two dimensions or the small-scale magnetic helicity to the turbulent diffusivity or the α

Table 1 Summary of results obtained over the years. The key to the references is given at the end of Sect. 1

Result	Details	Reference
$\eta_t \sim R_m^{-1}$	2-D periodic, $\overline{\mathbf{B}} \sim \sin kx$	CV91
$\alpha \sim R_m^{-1}$	phenomenology, $\langle \mathbf{A} \cdot \mathbf{B} \rangle$ conservation, simulations with $\overline{\mathbf{B}} = \text{const}$	VC92, GD94, CH96
$\overline{B}^2/B_{\text{eq}}^2 \sim R_m^{-1}$	helical turbulence, normal field b.c.	GD94, BD01
$\overline{B}^2/B_{\text{eq}}^2 \sim k_f/k_1$	helical turbulence, periodic domain	B01
$\overline{B}^2/B_{\text{eq}}^2 \gg k_f/k_1$	helical turb. with shear, periodic	BBS01, BB02
$\overline{B}^2/B_{\text{eq}}^2 \sim 0.5$	helical turb. with horizontal shear, normal field b.c.	B05
$\overline{B}^2/B_{\text{eq}}^2 \ll 0.5$	convection with vertical shear, normal field b.c.	TCB08
$\overline{B}^2/B_{\text{eq}}^2 \sim 0.5$	convection with horizontal shear, normal field b.c.	KKB08

effect in three dimensions. This can be done using a corresponding mean-field equation for these quantities.

The effect of such nonlinear dependencies of turbulent transport coefficients on the dynamo can be quite dramatic. In three dimensions, Gruzinov and Diamond (1995) showed that in the case of pseudo-vacuum boundary conditions the saturation field strength of a dynamo with just helicity is of the order of $R_m^{-1/2} B_{\text{eq}}$. This was also confirmed by simulations (Brandenburg and Dobler 2001, hereafter BD01; Brandenburg and Subramanian 2005a). In the special case of periodic boundary conditions, however, the field strength does not decline, but remains of the order of $(k_f/k_1)^{1/2} B_{\text{eq}}$ (Brandenburg 2001, hereafter B01). This is now well understood as being a consequence of magnetic helicity evolution, which was soon applied to cases with shear (Brandenburg et al. 2001, hereafter BBS01; Blackman and Brandenburg 2002, hereafter BB02) in domains with periodic as well as open boundary conditions (Brandenburg 2005, hereafter B05). Magnetic helicity evolution has also been invoked to understand recent simulations of convection by Tobias et al. (2008, hereafter; TCB08) and Käpylä et al. (2008a, hereafter KKB08).

Table 1 summarizes a number of results that have been obtained over the years. These results may appear conflicting at first sight, but they are in fact all explained by modern dynamo theory that takes magnetic helicity evolution into account, and that allows for magnetic helicity changes in the presence of losses through boundaries. In the following we restrict ourselves to cases in Cartesian geometry, but we note that important progress is now also being made in spherical shell geometry where large-scale fields have been seen when rotation is sufficiently rapid (Brown et al. 2007).

2 Saturation Phenomenology in a Periodic Box

During the early phase of a strongly helical dynamo there can be a phase during which the magnetic energy of the large-scale field is still subdominant. However, at later times the magnetic energy can redistribute itself from small to large scales. The fields that suffer minimal back-reaction from the Lorentz force tend to be force-free at large scales. Force-free fields are generally referred to as Beltrami fields. Qualitatively speaking, the helical driving produces a helical field at the driving scale, but because magnetic helicity cannot change, helical field of opposite helicity must emerge at some other scale. Simple arguments show that this can only happen at a larger scale (Frisch et al. 1975; see also Brandenburg and Subramanian 2005b). To explain the evolution of the resulting large-scale magnetic field, let

us begin with the evolution equation of magnetic helicity,

$$\frac{d}{dt} \langle \mathbf{A} \cdot \mathbf{B} \rangle = -2\eta\mu_0 \langle \mathbf{J} \cdot \mathbf{B} \rangle, \tag{1}$$

where angular brackets denote volume averages, η is the microscopic magnetic diffusivity, μ_0 is the vacuum permeability, and $\mathbf{J} = \nabla \times \mathbf{B} / \mu_0$ is the current density. Next, we introduce horizontal averages denoted by overbars. The direction over which we take these averages depends of course on the direction in which the mean magnetic field chooses to align itself. There are three equivalent possibilities, so let us assume that the field shows a large-scale modulation in the z direction. In a periodic box the Beltrami field with the smallest wavenumber is then of the form

$$\overline{\mathbf{B}} = \overline{\mathbf{B}}(z, t) = \hat{\mathbf{B}}(t) (\cos k_1 z, \sin k_1 z, 0), \tag{2}$$

where we have ignored the possibility of an arbitrary phase shift in the z direction. Note that $\overline{\mathbf{J}}(z, t) = -k_1 \overline{\mathbf{B}} / \mu_0$ and $\overline{\mathbf{A}}(z, t) = -k_1^{-1} \overline{\mathbf{B}}$, so the current and magnetic helicities have negative sign at large scales. This is the situation when the small-scale driving has positive helicity.

Note that the definition of averaging automatically defines small-scale (or fluctuating) magnetic fields as $\mathbf{b} = \mathbf{B} - \overline{\mathbf{B}}$, and likewise for $\mathbf{a} = \mathbf{A} - \overline{\mathbf{A}}$ and $\mathbf{j} = \mathbf{J} - \overline{\mathbf{J}}$. We can then split (1) into contributions from large scales and small scales, reorganize the equations in terms of $\langle \overline{\mathbf{B}}^2 \rangle$ and $\langle \mathbf{b}^2 \rangle$, assume that, after the end of the kinematic phase ($t = t_s$), $\langle \mathbf{b}^2 \rangle$ is approximately constant in time (approximately equal to $\mu_0 \langle \rho \mathbf{u}^2 \rangle$). This yields (B01)

$$k_1^{-1} \frac{d \langle \overline{\mathbf{B}}^2 \rangle}{dt} = 2\eta k_f \langle \mathbf{b}^2 \rangle - 2\eta k_1 \langle \overline{\mathbf{B}}^2 \rangle, \tag{3}$$

which has the solution

$$\langle \overline{\mathbf{B}}^2 \rangle = \langle \mathbf{b}^2 \rangle \frac{k_f}{k_1} \left[1 - e^{-2\eta k_1^2 (t-t_s)} \right]. \tag{4}$$

Thus, $\langle \overline{\mathbf{B}}^2 \rangle$ saturates on a time scale $(2\eta k_1^2)^{-1}$, i.e. the microscopic diffusion time based on the scale of the box. This equation reproduces extremely well the saturation behavior in a periodic box. This equation also shows what happens if either the fluctuating field or the mean field are not fully helical (Brandenburg et al. 2002). For example, if the large-scale field is no longer fully helical, then the ratio $\mu_0 |\langle \overline{\mathbf{J}} \cdot \overline{\mathbf{B}} \rangle| / \langle \overline{\mathbf{B}}^2 \rangle$ will be less than k_1 , so we say that the *effective* value of k_1 will be smaller. (Later on we refer to this value as k_m .) Thus, if the large-scale field is not fully helical, but the small-scale field is still fully helical, then the effective value of k_1 in the denominator of (4) decreases and $\langle \overline{\mathbf{B}}^2 \rangle$ can be even somewhat higher than for periodic boundary conditions. This is indeed the case for perfectly conducting boundary conditions, which do not permit (2) as a solution. This is the reason why the effective value of k_1 is smaller, and hence $\langle \overline{\mathbf{B}}^2 \rangle$ is larger (Brandenburg and Dobler 2002). Conversely, if the small-scale field is not fully helical, the effective value of k_f is smaller, and so $\langle \overline{\mathbf{B}}^2 \rangle$ is smaller (Maron and Blackman 2002; Brandenburg et al. 2002).

We emphasize that in the considerations in this section we did not invoke mean-field theory at all. The slow-down during the final saturation stage is rather general and it should be possible to describe this by a sufficiently detailed mean-field theory. This will be discussed briefly in the following section.

3 Mean-Field Theory and Transport Coefficients

In mean-field theory one considers the averaged induction equation. The cross-product of the correlation of the fluctuations $\mathbf{u} = \mathbf{U} - \overline{\mathbf{U}}$ and $\mathbf{b} = \mathbf{B} - \overline{\mathbf{B}}$, i.e. the mean electromotive force, $\overline{\mathcal{E}} = \overline{\mathbf{u} \times \mathbf{b}}$, provides an important term in the averaged induction equation,

$$\frac{\partial \overline{\mathbf{B}}}{\partial t} = \nabla \times (\overline{\mathbf{U}} \times \overline{\mathbf{B}} + \overline{\mathcal{E}} - \eta \mu_0 \overline{\mathbf{J}}). \tag{5}$$

A central goal of mean-field theory is to find expressions for $\overline{\mathcal{E}}$ in terms of mean-field quantities. Quadratic correlations such as $\overline{\mathcal{E}}$ are obtained using evolution equations for the fluctuations, $\mathbf{u} \equiv \mathbf{U} - \overline{\mathbf{U}}$ and $\mathbf{b} = \mathbf{B} - \overline{\mathbf{B}}$. A range of different approaches can be used to calculate the functional form of the mean electromotive force, $\overline{\mathcal{E}} = \overline{\mathbf{u} \times \mathbf{b}}$, including the second order correlation approximation (SOCA), the τ approximation, and the renormalization group procedure. Common to both the SOCA and the τ approximation is the fact that the linear terms in the evolution equations for the fluctuations are solved exactly. However, there is an important difference in that the τ approximation starts by computing the time evolution of $\overline{\mathcal{E}}$, so one begins with

$$\partial \overline{\mathcal{E}} / \partial t = \overline{\dot{\mathbf{u}} \times \mathbf{b}} + \overline{\mathbf{u} \times \dot{\mathbf{b}}}, \tag{6}$$

whereas under SOCA one uses primarily the induction equation by computing $\overline{\mathcal{E}} = \overline{\mathbf{u} \times \mathbf{b}}$, where \mathbf{u} is assumed given and \mathbf{b} is being solved using the Green's function for the induction equation. In simple terms, this reduces to solving for $\overline{\mathcal{E}} = \overline{\mathbf{u} \times \int \dot{\mathbf{b}} dt}$. This distinction is important because under the τ approximation the term $\overline{\dot{\mathbf{u}} \times \mathbf{b}}$ leads immediately to a term of the form $(\mathbf{j} \times \overline{\mathbf{B}}) \times \mathbf{b}$ owing to the Lorentz force. This expression leads to an important feedback by attenuating the α effect by a term α_M , where, under the assumption of isotropy, $\alpha_M = \frac{1}{3} \tau \overline{\mathbf{j} \cdot \mathbf{b}}$ is the magnetic α effect. Another important difference is that there is a natural occurrence of a time derivative of $\overline{\mathcal{E}}$. Thus, compared with SOCA, which leads to

$$\overline{\mathcal{E}}_i = \alpha_{ij} \overline{B}_j + \eta_{ijk} \overline{B}_{j,k}, \tag{7}$$

one now has

$$\tau \partial \overline{\mathcal{E}}_i / \partial t + \overline{\mathcal{E}}_i = \alpha_{ij} \overline{B}_j + \eta_{ijk} \overline{B}_{j,k}, \tag{8}$$

where τ is a relaxation time, and a comma between indices denotes a spatial derivative. In (8) the origin of the $\tau \partial \overline{\mathcal{E}} / \partial t$ term is clear in view of (6), and it is instead the $\overline{\mathcal{E}}$ term that is due to retaining nonlinear terms in the evolution equations for \mathbf{u} and \mathbf{b} . In both cases these terms lead to the triple correlations that are then approximated by $-\overline{\mathcal{E}}/\tau$ on the right hand side. After multiplying by τ , this leads to the \mathcal{E} term in (8).

In the expressions above we have used the more general tensorial forms of α effect and turbulent diffusion. Scalar transport coefficients used before denote the isotropic contributions of the α_{ij} and η_{ijk} tensors, i.e. $\alpha = \frac{1}{3} \delta_{ij} \alpha_{ij}$ and $\eta_t = \frac{1}{6} \epsilon_{ijk} \eta_{ijk}$.

Both SOCA and the τ approximation are rather primitive and their merits has been discussed in some detail in the recent literature (Rädler and Rheinhardt 2007; Sur et al. 2007). The emergence of the $\overline{\mathbf{j} \cdot \mathbf{b}}$ term is qualitatively a new feature that leads to a quantitative description of the saturation of large-scale dynamos in periodic domains (Field and Blackman 2002, BB02). Furthermore, the emergence of an additional time derivative in (8) has been confirmed qualitatively using simulations (Brandenburg et al. 2004). However, there is now

also evidence for the occurrence of even higher time derivatives in some cases (Hubbard and Brandenburg 2008).

The time derivative in (8) suppresses changes of mean-field properties on timescales shorter than the turnover time τ of the turbulence. This is analogous to the occurrence of the Faraday displacement current in the Maxwell equations, except that there the limiting velocity is the speed of light, whereas here it is the rms velocity of the turbulence. This changes the parabolic nature of the diffusion and dynamo equations into hyperbolic wave equations (Blackman and Field 2003; Brandenburg et al. 2004). This property is physically appealing, because it retains causality, which means here that no mean-field pattern can propagate faster than the rms velocity of the turbulence.

Similar to the suppression of fast temporal variations discussed above, there is also a suppression of spatial variations on short length scales. Indeed, (8) takes the more accurate form

$$\tau \partial \overline{\mathcal{E}}_i / \partial t + \overline{\mathcal{E}}_i = \hat{\alpha}_{ij} \circ \overline{B}_j + \hat{\eta}_{ijk} \circ \overline{B}_{j,k}, \tag{9}$$

where $\hat{\alpha}_{ij}$ and $\hat{\eta}_{ijk}$ are the components of integral kernels and the circles denote a convolution. Recent numerical work has now established that for driven turbulence the integral kernels have an exponential form with a width given by the inverse wavenumber of the energy-carrying eddies (Brandenburg et al. 2008b).

This implies that mean-field theory should never produce rapid spatial or temporal variations. Conversely, the more complicated kernel formulation in (9) can be avoided if the solutions are sufficiently smooth in space and time. However, this is not always guaranteed, especially near boundaries.

Let us at this point also highlight the occurrence of another time derivative in the mean-field equations. Under the τ approximation, the $(\mathbf{j} \times \overline{\mathbf{B}}) \times \mathbf{b}$ term leads to the emergence of a magnetic contribution to the α effect. The full α effect is then written as $\alpha = \alpha_K + \alpha_M$, where α_K is related to the kinetic helicity and α_M is related to the current helicity. The latter obeys an evolution equation where the omission of the time-derivative is often problematic, especially when R_m is large and the mean divergence of current helicity fluxes vanishes. Therefore, the more complete quenching formula with extra effects included takes the form (see, e.g., Brandenburg 2008),

$$\alpha = \frac{\alpha_0 + R_m \left(\eta_t \frac{\mu_0 \overline{\mathbf{J}} \cdot \overline{\mathbf{B}}}{B_{\text{eq}}^2} - \frac{\nabla \cdot \overline{\mathcal{F}}_C}{2k_t^2 B_{\text{eq}}^2} - \frac{\partial \alpha / \partial t}{2\eta_t k_t^2} \right)}{1 + R_m \overline{\mathbf{B}}^2 / B_{\text{eq}}^2}. \tag{10}$$

Although this equation can be written as an evolution equation, in practice there is a computational advantage in solving the time-derivative term implicitly; see Brandenburg and Käpylä (2007). The properties of such a “dynamical” α quenching formula have been studied in a number of recent papers including Kleorin et al. (2000), Field and Blackman (2002), BB02, and Brandenburg and Subramanian (2005a).

4 The Test-Field Method

In the last few years a new and reliable method for calculating the α_{ij} and η_{ijk} tensor coefficients has become available. This method is known as the test-field method and was developed by Schrunner et al. (2005, 2007) to calculate all tensor components from snapshots of simulations of the geodynamo in a spherical shell. This method was later applied

to time-dependent turbulence in triply-periodic Cartesian domains, both with shear and no helicity (Brandenburg 2005; Brandenburg et al. 2008a) as well as without shear, but with helicity (Sur et al. 2008; Brandenburg et al. 2008b), and also with both (Mitra et al. 2008a).

4.1 The Essence of the Test-Field Method

In the test-field method one solves an additional set of three-dimensional partial differential equations for vector fields \mathbf{b}^{pq} , where the labels $p = 1, 2$ and $q = 1, 2$ correspond to different pre-determined one-dimensional test fields $\overline{\mathbf{B}}^{pq}$. The evolution equations for \mathbf{b}^{pq} are derived by subtracting the mean-field evolution equation from the evolution equation for \mathbf{B} . These equations are *distinct* from the original induction equation in that the curl of the resulting mean electromotive force is subtracted.

The test-field method has recently been criticized by Cattaneo and Hughes (2008) on the grounds that the test fields are arbitrary pre-determined mean fields. They argue that the resulting turbulent transport coefficients will only be approximations to the true values unless the test fields are close to the actual mean fields. Mitra et al. (2008a) have reviewed arguments supporting the validity of the test-field method: (i) the test-field method correctly reproduces a vanishing growth rate in saturated nonlinear cases (Brandenburg et al. 2008c); (ii) in the time-dependent case, the test-field method correctly reproduces also a non-vanishing growth rate. In that case one must write (7) as a convolution in time (Hubbard and Brandenburg 2008); (iii) for the Roberts flow with a mean field of Beltrami type, the α_{ij} tensor is anisotropic and has an additional component proportional to $\overline{B_i B_j}$ that tends to quench the components of the isotropic part of α_{ij} . The same α_{ij} tensor also governs the evolution of a mean passive vector field. It turns out that the fastest growing passive vector field is then phase-shifted by 90 degrees relative to the one that caused the quenching and thus the quenched form of α_{ij} . This result has been confirmed both numerically and using weakly nonlinear theory (Tilgner and Brandenburg 2008). We discuss this case further in Sect. 4.4.

4.2 R_m -Dependence of the Kinematic Values of α and η_t

Using the test-field method it has, for the first time, become possible to obtain reliable estimates not only for the α effect, but in particular also for the turbulent magnetic diffusivity. Restricting ourselves to the case of horizontal (xy) averages, the mean fields depend only on z and t . All components of $\overline{B_{j,k}}$ can therefore be expressed in terms of those of $\overline{\mathbf{J}}(z, t)$, and the relevant components of η_{ijk} reduce to a rank-2 tensor, η_{ij} . In that case, $\eta_t = \frac{1}{2}(\eta_{11} + \eta_{22})$. We present the R_m dependences of α and η_t in normalized forms using the SOCA results for homogeneous isotropic turbulence as reference values,

$$\alpha_0 = -\frac{1}{3}\tau\overline{\boldsymbol{\omega} \cdot \mathbf{u}}, \quad \eta_{t0} = \frac{1}{3}\tau\overline{\mathbf{u}^2} \quad (\text{SOCA, linear}). \tag{11}$$

It turns out that, in the kinematic regime, α_0 and η_{t0} are remarkably close to the numerically determined values of α and η_t in the range $1 < R_m < 200$ considered in the study of Sur et al. (2008); see Fig. 1. For $R_m < 1$, both α and η_t increase linearly with R_m . In the cases considered here we have assumed that the turbulence is fully helical, so $\overline{\boldsymbol{\omega} \cdot \mathbf{u}} \approx k_f \overline{\mathbf{u}^2}$, and that the Strouhal number, $St \equiv \tau u_{\text{rms}} k_f$ is approximately equal to unity (Brandenburg and Subramanian 2005c, 2007). Of course, for $R_m < 1$ this is not the case and then $\tau \approx (\eta k_f^2)^{-1}$ is a better estimate. This explains the linear increase of α and η_t for $R_m < 1$.

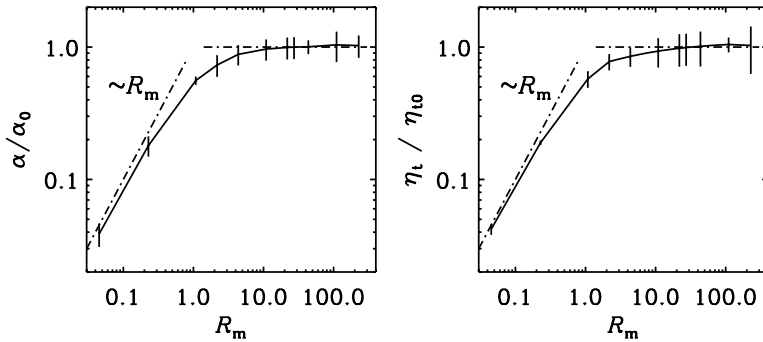


Fig. 1 Dependence of the normalized values of α and η_t on R_m for $Re = 2.2$. The vertical bars denote twice the error estimated by averaging over subsections of the full time series. The run with $R_m = 220$ ($Re = 2.2$) was done at a resolution of 512^3 meshpoints. Adapted from Sur et al. (2008)

4.3 Scale-Dependence of α and η_t

Using the test-field method, it has now also been possible to determine what happens if there is poor scale separation, for example if the scale of the mean field is only 2–5 times bigger than the scale of the energy-carrying eddies. In that case one can not longer write the electromotive force in terms of products of α and the mean field or η_t and the mean current density, but one has to write them as convolutions with corresponding integral kernels (e.g. Brandenburg and Sokoloff 2002). In Fourier space, a convolution corresponds to a multiplication. In the test-field method we use only harmonic test fields with a single wavenumber, so we can use this method to calculate α and η_t separately for each wavenumber and obtain the integral kernels via Fourier transformation.

Not surprisingly, it turns out that α and η_t decrease with decreasing scale, i.e. with increasing values of k/k_f , where k is the wavenumber of a particular Fourier mode of the field. In fact, by calculating α and η_t for test-fields of different wavenumber k , one finds that for isotropic turbulence, α and η_t have Lorentzian profiles of the form

$$\alpha(k) = \frac{\alpha_0}{1 + (a_\alpha k/k_f)^2}, \quad \eta_t(k) = \frac{\eta_{t0}}{1 + (a_\eta k/k_f)^2}, \tag{12}$$

where a_α and a_η are factors of order unity; Brandenburg et al. (2008b) find $a_\alpha \approx 1$ and $a_\eta \approx 0.5$. However, for shear-flow turbulence Mitra et al. (2008a) find $a_\alpha \approx a_\eta \approx 0.7$.

In periodic domains the Fourier transforms of $\alpha(k)$ and $\eta_t(k)$ correspond to the integral kernels introduced in (9). They are of exponential form, i.e.,

$$\hat{\alpha}(z - z') = \frac{1}{2} a_\alpha \alpha_0 k_f \sim \exp(-k_f |z - z'| / a_\alpha) \tag{13}$$

and

$$\hat{\eta}_t(z - z') = \frac{1}{2} a_\eta \eta_{t0} k_f \sim \exp(-k_f |z - z'| / a_\eta). \tag{14}$$

It is important to realize that the test-field method is a tool to analyze the velocity field that is giving rise to α and η_t effects. By applying the test-field method to the case where the induction equation is solved together with the momentum and continuity equations, one can analyze the nonlinear case for one specific value of $\overline{\mathbf{B}}$. We emphasize that the test field does not enter the momentum equation in any way. This will be discussed next.

4.4 Quenching for Equipartition-Strength Fields

Once the magnetic field has become sufficiently strong, α and η_t will become anisotropic, even though the turbulence was originally isotropic. If the anisotropy is only due to $\overline{\mathbf{B}}$, the tensors α_{ij} and η_{ijk} are of the form

$$\alpha_{ij}(\overline{\mathbf{B}}) = \alpha_1(\overline{\mathbf{B}})\delta_{ij} + \alpha_2(\overline{\mathbf{B}})\widehat{B}_i\widehat{B}_j, \tag{15}$$

$$\eta_{ij}(\overline{\mathbf{B}}) = \eta_1(\overline{\mathbf{B}})\delta_{ij} + \eta_2(\overline{\mathbf{B}})\widehat{B}_i\widehat{B}_j, \tag{16}$$

where $\widehat{\mathbf{B}} = \overline{\mathbf{B}}/|\overline{\mathbf{B}}|$ is the unit vector of the mean field.

For equipartition-strength fields, $|\overline{\mathbf{B}}| = O(B_{eq})$, the R_m dependence of α_1 , α_2 , η_1 , and η_2 has been determined by Brandenburg et al. (2008c). It turns out that α_1 and α_2 have opposite signs (Fig. 2), so when α_{ij} is applied to the actual mean field we have

$$\alpha_{ij}B_j = (\alpha_1 + \alpha_2)B_i. \tag{17}$$

This shows that the α effect is magnetically quenched by the suppressing effect of α_2 on α_1 due to its opposite sign. However, even though the value of $\alpha_1 + \alpha_2$ decreases with increasing values of R_m , it is only quenched down to values comparable to the value of η_1k_1 if $|\overline{\mathbf{B}}| = O(B_{eq})$; see Fig. 2. This becomes obvious by looking at the expression for the linear growth rate,

$$\lambda = (\alpha_1 + \alpha_2)k_m - (\eta + \eta_1 + \eta_2)k_m^2, \tag{18}$$

where $k_m = \mu_0\langle\overline{\mathbf{J}} \cdot \overline{\mathbf{B}}\rangle/\langle\overline{\mathbf{B}}^2\rangle$ is the effective wavenumber of the mean field. We note however that the use of λ is only permissible because $\overline{\mathbf{B}}^2$ and $\overline{\mathbf{J}} \cdot \overline{\mathbf{B}}$ are spatially uniform for α^2 dynamos in a periodic domain. For a forcing function with positive helicity we have $k_f > 0$, and so $k_m < 0$. Moreover, for fully helical mean fields we have $k_m = -k_1$. In the saturated state, the growth rate must be zero, which means then that $\alpha_1 + \alpha_2$ must become comparable to $(\eta + \eta_1 + \eta_2)k_m$.

The occurrence of the $\widehat{B}_i\widehat{B}_j$ term in (15) and the negative sign of α_2/α_1 have been confirmed independently by observing that the velocity field of a saturated dynamo can itself lead to dynamo action for a passive vector field obeying a kinematic induction equation.

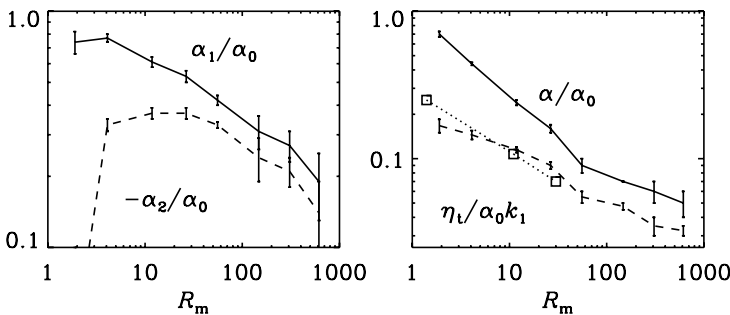


Fig. 2 R_m dependence of α_1 and $-\alpha_2$ (left) and of α and $\eta_t k_1$ (right) for equipartition-strength fields, $|\overline{\mathbf{B}}| = O(B_{eq})$. The mutual approach of α_1 and $-\alpha_2$ illustrates how α quenching is accomplished, and the mutual approach of α and $\eta_t k_1$ illustrates by how much the quenching has to proceed

Such an observation was first made by Cattaneo and Tobias (2008) in a convection-driven small-scale dynamo and later by Tilgner and Brandenburg (2008) for the Roberts (1972) flow dynamo, where $\mathbf{u} = k_f \psi \hat{z} + \nabla \times \psi \hat{z}$ with $\psi = (u_0/k_1) \cos k_1 x \cos k_1 y$ and $k_f = \sqrt{2}k_1$. As in the case of helical isotropic turbulence in a triply-periodic domain the solutions for $\overline{\mathbf{B}}$ are also here Beltrami fields of the form $\overline{\mathbf{B}} = (\cos k_1 z, \sin k_1 z, 0)$, where k_0 is the horizontal wavenumber of the helices of the Roberts flow.

The resulting matrix $\overline{B}_i \overline{B}_j$ has eigenvalues 1 and 0. In the saturated state, the eigenfunction corresponding to eigenvalue 0 is $\tilde{\overline{\mathbf{B}}} = (\sin k_1 z, -\cos k_1 z, 0)$ and has the growth rate $\lambda = \alpha_1(\overline{\mathbf{B}})k_1 - [\eta_1(\overline{\mathbf{B}}) + \eta]k_1^2$, which is positive, even after $\overline{\mathbf{B}}$ has reached saturation. This corresponds to continued exponential growth of $\tilde{\overline{\mathbf{B}}}$, which confirms the original finding based on the test-field method.

The results obtained using the test-field methods should of course be of predictive value to be useful. The application to a passive vector field discussed above is one example where the result for the full nonlinear α tensor was used to predict the evolution of the passive vector field. Another example is the case of rigidly rotating convection. Using the test-field method, Käpylä et al. (2008b) noticed that with increasing rotation rate α increases and η_t decreases. This led to the prediction that there should be α^2 dynamo action (i.e. without any shear!) for sufficiently rapid rotation. This was later confirmed using direct simulations (Käpylä et al. 2008c).

5 Three Paradigm Shifts Revisited

Let us now turn attention to the Sun. Solar dynamo theory has experienced arguably three major paradigm shifts since its broad initial acceptance during the 1970s. Inevitably, these paradigm shifts have brought the modelling further away from the original ideas that were based on dynamo theory. At the same time solar dynamo theory has lost much of its initial rigor that dynamo theory used to be based on, i.e. the profiles of α and η_t are no longer calculated, but are considered freely adjustable. The same is true of the magnetic quenching properties of these profiles. It is therefore important that the motivation for such departures from the original theory are well justified. In the following we discuss and comment on each of the three paradigm shifts.

5.1 Magnetic Buoyancy: from Distributed Dynamos to the Overshoot Layer

In an influential paper by Spiegel and Weiss (1980), a number of different aspects led to the suggestion that the solar dynamo operates at the base of the convection zone. One of the arguments concerned the rapid rise of magnetic flux tubes from the bulk of the convection zone. Subsequent simulations, however, have demonstrated a strongly opposing effect due to turbulent magnetic pumping (Brandenburg and Tuominen 1991; Nordlund et al. 1992; Brandenburg et al. 1996; Tobias et al. 1998). It appears, therefore, that magnetic buoyancy might not constitute a problem for the dynamo, even though its effects are clearly visible in regions where the field is strong. An example is Fig. 10 of Brandenburg et al. (1996), where the strongest tube is just “hovering” at the same height in a balance between magnetic buoyancy and downward pumping.

5.2 Helioseismology: Overshoot Layer and Flux-Transport Dynamos

The idea of dynamos operating in the overshoot layer was soon reinforced when it became evident that in the bulk of the convection zone the *radial* differential rotation, which is

important for the mean-field dynamo, is small. At the time, the strongest shear was believed to occur at the bottom of the convection zone. The positive value of the radial differential rotation in this layer, which is now called the tachocline, together with an α effect of opposite sign relative to what it is in the bulk of the convection zone, could explain the equatorward migration of the sunspot belts (DeLuca and Gilman 1986, 1988; Rüdiger and Brandenburg 1995). However, as with all models that have a positive radial angular velocity gradient, also these models have the wrong phase relation, i.e. the radial and toroidal mean fields are in phase and not in antiphase, as observed (Yoshimura 1976; Stix 1976). However, the phase relation may not pose a serious problem (Schüssler 2005).

Another possibility is that the dynamo could operate with spatially disjoint induction layers: an α effect with the usual sign near the surface, and positive radial shear at the bottom of the convection zone, coupled by meridional circulation. This led to the now popular idea of flux-transport dynamos where the meridional circulation is chiefly responsible for the equatorward migration of the toroidal flux belts (see Dikpati and Gilman 2009). However, in recent years it became clear that in the outer 5% of the Sun by radius there is strong negative radial shear (Benevolenskaya et al. 1999), which could in principle also explain the equatorward migration in the framework of conventional solar dynamo theory (B05). On the other hand, such a theory also faces problems of its own, for example the latitudinal width of the flux belts is expected to be only a few times bigger than the depths of the supergranulation layer (Brandenburg and Käpylä 2007), which would be too small.

5.3 Catastrophic Quenching: Interface and Flux-Transport Dynamos

The possibility of catastrophic quenching led Parker (1993) to propose the so-called interface dynamo where the magnetic field would be weak in the bulk of the convection zone, so as to avoid catastrophic quenching. However, as discussed in the present paper, catastrophic quenching is *always* a serious possibility, even for interface dynamo, which means that magnetic helicity fluxes are needed to alleviate it. One might well imagine that it is easier to shed magnetic helicity when the dynamo operates closer to the surface. Such models have not yet been investigated in sufficient detail.

In conclusion, there are now reasons to believe that all three paradigm shifts are problematic and may need to be reconsidered. An alternative proposal would be that the solar dynamo operates in the bulk of the convection zone, just as anticipated originally in the 1970s, and that the near-surface shear layer may play an important role in shaping the solar dynamo wave (B05).

6 Implications and Open Problems

In future work it will be important to improve our understanding of the solar dynamo, in particular its location within the Sun, its 22 year period, and the origin of the equatorward migration of the sunspot belts. As discussed in the previous section, current thinking places the solar dynamo in the tachocline, i.e. the bottom of the convection zone where the internal angular velocity turns from nearly uniform in the interior to non-uniform in the convection zone. The idea is that the field strength there exceeds the equipartition value by a factor of 100 (D'Silva and Choudhuri 1993), but such a strong field has not yet been reported based on turbulent three-dimensional dynamo simulations. Observationally not much can be said yet, because such fields would be below current helioseismological detection limits. On the theoretical side, a serious problem is that one assumes a turbulent magnetic Prandtl number

of 100, instead of 1, which is predicted by theory and simulations (Yousef et al. 2003). Such considerations neglect however the turbulent viscosity associated with the Maxwell stress of small-scale magnetic fields. Clearly, any *ad hoc* modifications of the theory are the result of trying to make the models reproduce the observations. However, at the same time such models ignore some important findings regarding the nonlinear behavior of the mean-field dynamo effect at large magnetic Reynolds numbers. Recent research has provided new detailed insights that should be followed up using more realistic settings such as spherical shell geometry.

There are several mechanisms proposed for explaining the cause of the equatorward migration of magnetic activity belts at low solar latitudes. Is it the rather feeble meridional circulation, as assumed in the now popular flux transport models (Dikpati and Charbonneau 1999), even though one has to assume unrealistic values of the *turbulent* magnetic Prandtl number, or is it perhaps the near-surface shear layer, which would have indeed the right sign, as emphasized in B05. To clarify things, future research may proceed along two parallel strands; one is connected with the development and exploitation of models in spherical geometry, and the other one is connected with unresolved problems that can be addressed in Cartesian configurations. In the following we list detailed steps of future research.

Catastrophic quenching in spherical shells. Catastrophic quenching behavior has still not yet been demonstrated convincingly in closed spheres or spherical shell sectors using, e.g., perfectly conducting boundary conditions and forced turbulence. Some work in this direction has already been done (Brandenburg et al. 2007; Mitra et al. 2008b), but the resolution is limited and the results not yet entirely conclusive.

Testfield method in spherical geometry. The test-field method needs to be re-examined in spherical coordinates. Originally the test-field method was developed in connection with full spheres, and then the test fields consisted of field components of constant value or constant slope. However, only afterwards it became clear that the scale (or wavenumber) of the field components must be the same for one set of all tensor components, and so it is necessary to work with spherical harmonic functions as test fields. In other words, constant and linearly varying field components are problematic.

Dynamo in open shells with and without shear. To verify our understanding of the saturation process of large-scale dynamos it is important to calculate, at different magnetic Reynolds numbers, the late stages of magnetic field evolution with open boundary conditions in spherical shells or shell sectors with and without shear. One expects low saturation amplitudes with energies of the mean magnetic field being inversely proportional to the magnetic Reynolds number in the absence of shear, but of order unity in the presence of shear. The shear is here critical, because shear is responsible for the local driving of small-scale magnetic helicity fluxes (Vishniac and Cho 2001; Subramanian and Brandenburg 2004, 2006).

Alpha effect from convection. The calculation of the α effect in convective turbulence is at the moment unclear. For unstratified convection with an imposed field Cattaneo and Hughes (2006) find that α diminishes for large magnetic Reynolds numbers, even for kinematically weak magnetic fields. With stratification, on the other hand, Käpylä et al. (2008b) find values of α that are compatible with those from simple estimates. They used the test-field method while Cattaneo and Hughes (2006) used an imposed field and estimate α as the ratio between the resulting field-aligned electromotive force and the imposed field. However, at large magnetic Reynolds number there is dynamo action producing also a mean field that might exceed the imposed field and thereby modify the estimate for α . Another possible reason for the discrepancy could be related to the presence or absence of stratification, because α is expected to be proportional to the local gradient of density and turbulent velocity

(Steenbeck et al. 1966). In unstratified Boussinesq convection the density is constant and the turbulent velocity only changes near boundaries. However, boundary effects could contribute to driving an α effect (Giesecke et al. 2005). Another problem could be poor scale separation, in which case the electromotive force is not just proportional to α and it becomes mandatory to use the integral kernel formulation instead (Brandenburg et al. 2008b).

Convective dynamos in spherical shells are now widely studied (Brun et al. 2004; Browning et al. 2006; Brown et al. 2007). It would be useful to compare the resulting magnetic fields with corresponding forced turbulence simulations in spherical shells and see whether contact can be made with improved mean-field models. This may require careful considerations of the scale-dependence of the turbulent transport coefficients.

Dynamos driven by magnetic instabilities. There is now quite a number of studies looking at possibilities where the flows driving the dynamo are due to the resulting magnetic field itself, and are driven by magnetic instabilities. Examples include magnetic buoyancy instabilities and the magneto-rotational instability. For example, the turbulence in accretion discs is believed to be driven by the magnetorotational instability. This was one of the first examples showing cyclic dynamo action somewhat reminiscent of the solar dynamo (Brandenburg et al. 1995), and it was believed to be a prototype of magnetically driven dynamos (Brandenburg and Schmitt 1998; Rüdiger and Pipin 2000; Rüdiger et al. 2001; Blackman and Field 2004). In the mean time, another example of a magnetically driven dynamo has emerged, where magnetic buoyancy works in the presence of shear and stratification alone (Brummell et al. 2002; Cline et al. 2003a, 2003b; Cattaneo et al. 2006). This phenomenon may be superficially similar to a magnetically dominated version of the shear-current effect (Rogachevskii and Kleeorin 2003, 2004). With the test-field method one is now in a good position to identify the governing mechanism by determining all components of the α and η_i tensors.

Magnetic flux concentrations near the surface. In the conventional picture, active regions and sunspots are thought to emerge as a result of magnetic flux tubes breaking through the surface. Given that it is difficult to imagine such tubes rising unharmed all the way from the bottom of the convection zone over so many pressure scale heights, one must test alternative scenarios in which the emergence of active regions and sunspots can be explained as the result of flux concentrations from local dynamo action via negative turbulent magnetic pressure effects (Kleeorin and Rogachevskii 1994) or turbulent flux collapse (Kitchatinov and Mazur 2000). Clearly, the underlying effects need to be established numerically and corresponding mean-field models need to be solved to make direct contact with simulations.

CME-like features above the surface. Given that virtually all successful large-scale dynamos at large magnetic Reynolds numbers are now believed to shed small-scale magnetic helicity, it is important to analyze the nature of the expelled magnetic field in simulations that couple to a simplified version of the lower solar wind. It is possible that the magnetic field above the surface and in the lower part of the solar wind might resemble coronal mass ejections (CMEs), in which case more detailed comparisons with actual coronal mass ejections would be beneficial.

Solar cycle forecast. Among the popular applications of solar dynamo theory and solar magnetohydrodynamics are solar cycle predictions, solar subsurface weather, and space weather. Also of interest are predictions of solar activity during its first 500 thousand years. This has great relevance for predicting the loss of volatile elements from the Earth's atmosphere, for example, and for understanding the conditions on Earth during the time when life began colonizing the planet. In this connection it is important to calculate the deflection of cosmic ray particles by the Sun's magnetic field and on the scale of the galaxy which is relevant for galactic cosmic rays (Svensmark 2007a, 2007b). However, such studies would

not be very meaningful unless some of the earlier projects in this list have resulted in a solar dynamo model that is trustworthy from a theoretical and a practical viewpoint.

Applications to laboratory liquid sodium dynamos. Unexpected beneficial insights have come from recent laboratory dynamo experiments. Unlike numerical dynamos, experimental liquid metal dynamos are able to address the regime of rather low values of the magnetic Prandtl number of the order of 10^{-5} , which is interesting in connection with solar and stellar conditions. At the same time the magnetic Reynolds number can be large enough (above 100) to allow for dynamo action. The Cadarache experiment is particularly interesting. Simulations of such a flow have been attempted by various groups using the Taylor-Green flow as a model (Ponty et al. 2004, 2005; Mininni et al. 2005; Brandenburg and Käpylä 2007). Again, the nature of the resulting dynamo effect has not yet been elucidated. It would be useful to analyze the resulting flows using the test-field method. One may hope that such work can teach us important lessons about large-scale and small-scale dynamos at low magnetic Prandtl number (Schekochihin et al. 2005; Iskakov et al. 2007), which is relevant to the Sun, but hard to address numerically with the currently available computing capabilities. Another relevant application is precession-driven dynamos (Tilgner 1999), where it might be useful to consider this process for a range of different geometries.

7 Conclusions

Looking back at some of the problems that dynamo theory was facing during the early years, we can say that a good deal of them have now been solved. For example the issue of turbulent magnetic diffusivity at large magnetic Reynolds numbers has now been addressed rather convincingly for values of R_m up to 200. Such a result has only recently become possible with the development of the test-field method. At this point we have no evidence that this result may change for larger values of R_m . Similar statements can be made about α , where it is now reasonably clear that in the *kinematic* regime α approaches a constant value for $1 \leq R_m \leq 200$. It should be emphasized that these results hold for forced turbulence and one must expect them to be different in cases of naturally forced turbulence such as convection or flows driven by magnetic instabilities such as the magneto-rotational instability (Brandenburg 2008) or the magnetic buoyancy instability (Brandenburg and Schmitt 1998; Thelen 2000).

Much larger values of R_m of 2×10^5 have been obtained for the special case of the Galloway-Proctor flow for which α shows irregular sign changes with R_m (Courvoisier et al. 2006). This flow is a time-dependent version of the Roberts flow where the pattern wobbles in the plane with given amplitude and frequency. Expressions of the form (11) do not apply in this case where the correlation time is infinite (Rädler and Brandenburg 2009). In that sense the Galloway-Proctor flow is quite different from a turbulent flow. Asymptotic behavior for large R_m is only possible for sufficiently large amplitude and/or frequency of the wobbling motion.

In the nonlinear case equally dramatic progress has been made in just the past few years. While it has long been clear that in closed domains α will be quenched down to values that depend on the quenched value of η_t and on the effective wavenumber of the mean field, it remained unclear what the quenched value of η_t is. Recent evidence points to a suppression by a factor of 5 when R_m is increased from 2 to 600 (Brandenburg et al. 2008c). However, this value may depend on circumstances and could be slightly less strong in the presence of shear (Käpylä and Brandenburg 2008).

In open domains there is the possibility that the resulting magnetic field strength can still decrease to catastrophically quenched values unless there is a finite divergence of the magnetic helicity flux (Brandenburg and Subramanian 2005a). Such a flux can be driven efficiently in the presence of shear. In order for this mechanism to operate, the contours of constant shear velocity must cross the boundaries (KKB08, Hughes and Proctor 2009), which explains the lack of large-scale fields in simulations with horizontal shear and periodic boundary conditions in that direction (Tobias et al. 2008).

There is clearly a long way to go before the solar dynamo problem can be addressed in full. There is hardly any doubt that the inclusion of magnetic helicity fluxes will be important, but the precise functional form of the magnetic helicity flux needs to be confirmed numerically. In particular, the possible dependencies of the fluxes on $\overline{\mathbf{B}}$ and R_m are not well understood at present.

Acknowledgements I would like to acknowledge Sasha Kosovichev and the other members of the team on Subphotospheric Dynamics of the Sun at the International Space Science Institute in Bern for providing an inspiring atmosphere. This work was supported in part by the Swedish Research Council.

References

- E.E. Benevolenskaya, J.T. Hoeksema, A.G. Kosovichev, P.H. Scherrer, The interaction of new and old magnetic fluxes at the beginning of solar cycle 23. *Astrophys. J.* **517**, L163–L166 (1999)
- E.G. Blackman, A. Brandenburg, Dynamic nonlinearity in large scale dynamos with shear. *Astrophys. J.* **579**, 359–373 (2002)
- E.G. Blackman, G.B. Field, A simple mean field approach to turbulent transport. *Phys. Fluids* **15**, L73–L76 (2003)
- E.G. Blackman, G.B. Field, Dynamical magnetic relaxation: A nonlinear magnetically driven dynamo. *Phys. Plasmas* **11**, 3264–3269 (2004)
- A. Brandenburg, The inverse cascade and nonlinear alpha-effect in simulations of isotropic helical hydro-magnetic turbulence. *Astrophys. J.* **550**, 824–840 (2001)
- A. Brandenburg, The case for a distributed solar dynamo shaped by near-surface shear. *Astrophys. J.* **625**, 539–547 (2005)
- A. Brandenburg, The dual role of shear in large-scale dynamos. *Astron. Nachr.* **329**, 725–731 (2008)
- A. Brandenburg, W. Dobler, Large scale dynamos with helicity loss through boundaries. *Astron. Astrophys.* **369**, 329–338 (2001)
- A. Brandenburg, W. Dobler, Hydromagnetic turbulence in computer simulations. *Comp. Phys. Comm.* **147**, 471–475 (2002)
- A. Brandenburg, P.J. Käpylä, Magnetic helicity effects in astrophysical and laboratory dynamos. *New J. Phys.* **9**, 305 (2007)
- A. Brandenburg, D. Schmitt, Simulations of an alpha-effect due to magnetic buoyancy. *Astron. Astrophys.* **338**, L55–L58 (1998)
- A. Brandenburg, D. Sokoloff, Local and nonlocal magnetic diffusion and alpha-effect tensors in shear flow turbulence. *Geophys. Astrophys. Fluid Dyn.* **96**, 319–344 (2002)
- A. Brandenburg, K. Subramanian, Strong mean field dynamos require supercritical helicity fluxes. *Astron. Nachr.* **326**, 400–408 (2005a)
- A. Brandenburg, K. Subramanian, Astrophysical magnetic fields and nonlinear dynamo theory. *Phys. Rep.* **417**, 1–209 (2005b)
- A. Brandenburg, K. Subramanian, Minimal tau approximation and simulations of the alpha effect. *Astron. Astrophys.* **439**, 835–843 (2005c)
- A. Brandenburg, K. Subramanian, Simulations of the anisotropic kinetic and magnetic alpha effects. *Astron. Nachr.* **328**, 507–512 (2007)
- A. Brandenburg, I. Tuominen, The solar dynamo, in *The Sun and Cool Stars: Activity, Magnetism, Dynamos*, *IAU Coll. 130*, ed. by I. Tuominen, D. Moss, G. Rüdiger. Lecture Notes in Physics, vol. 380 (Springer, Berlin, 1991), pp. 223–233
- A. Brandenburg, J.L. Jennings, Å. Nordlund, M. Rieutord, R.F. Stein, I. Tuominen, Magnetic structures in a dynamo simulation. *J. Fluid Mech.* **306**, 325–352 (1996)

- A. Brandenburg, A. Bigazzi, K. Subramanian, The helicity constraint in turbulent dynamos with shear. *Mon. Not. R. Astron. Soc.* **325**, 685–692 (2001)
- A. Brandenburg, W. Dobler, K. Subramanian, Magnetic helicity in stellar dynamos: new numerical experiments. *Astron. Nachr.* **323**, 99–122 (2002)
- A. Brandenburg, P.J. Käpylä, D. Mitra, D. Moss, R. Tavakol, The helicity constraint in spherical shell dynamos. *Astron. Nachr.* **328**, 1118–1121 (2007)
- A. Brandenburg, P. Käpylä, A. Mohammed, Non-Fickian diffusion and tau-approximation from numerical turbulence. *Phys. Fluids* **16**, 1020–1027 (2004)
- A. Brandenburg, D. Moss, A.M. Soward, New results for the Herzenberg dynamo: steady and oscillatory solutions. *Proc. R. Soc. A* **454**, 1283–1300 (1998)
- A. Brandenburg, Å. Nordlund, R.F. Stein, U. Torkelsson, Dynamo generated turbulence and large scale magnetic fields in a Keplerian shear flow. *Astrophys. J.* **446**, 741–754 (1995)
- A. Brandenburg, K.-H. Rädler, M. Rheinhardt, P.J. Käpylä, Magnetic diffusivity tensor and dynamo effects in rotating and shearing turbulence. *Astrophys. J.* **676**, 740–751 (2008a)
- A. Brandenburg, K.-H. Rädler, M. Schrunner, Scale dependence of alpha effect and turbulent diffusivity. *Astron. Astrophys.* **482**, 739–746 (2008b)
- A. Brandenburg, K.-H. Rädler, M. Rheinhardt, K. Subramanian, Magnetic quenching of alpha and diffusivity tensors in helical turbulence. *Astrophys. J. Lett.* **687**, L49–L52 (2008c)
- B.P. Brown, M.K. Browning, A.S. Brun, M.S. Miesch, N.J. Nelson, J. Toomre, Strong dynamo action in rapidly rotating suns. *AIPC* **948**, 271–278 (2007)
- M.K. Browning, M.S. Miesch, A.S. Brun, J. Toomre, Dynamo action in the solar convection zone and tachocline: pumping and organization of toroidal fields. *Astrophys. J.* **648**, L157–L160 (2006)
- N. Brummell, K. Cline, F. Cattaneo, Formation of buoyant magnetic structures by a localized velocity shear. *Mon. Not. R. Astron. Soc.* **329**, L73–L76 (2002)
- A.S. Brun, M.S. Miesch, J. Toomre, Global-scale turbulent convection and magnetic dynamo action in the solar envelope. *Astrophys. J.* **614**, 1073–1098 (2004)
- F. Cattaneo, D.W. Hughes, Nonlinear saturation of the turbulent alpha effect. *Phys. Rev. E* **54**, R4532–R4535 (1996)
- F. Cattaneo, D.W. Hughes, Dynamo action in a rotating convective layer. *J. Fluid Mech.* **553**, 401–418 (2006)
- F. Cattaneo, D.W. Hughes, Problems with kinematic mean field electrodynamics at high magnetic Reynolds numbers (2008). [arXiv:0805.2138](https://arxiv.org/abs/0805.2138)
- F. Cattaneo, S.M. Tobias, How do dynamos saturate? *J. Fluid Mech.* (2008). [arXiv:0809.1801](https://arxiv.org/abs/0809.1801). See also the talk given at the Kavli Institute for Theoretical Physics “Large and small-scale dynamo action” (http://online.kitp.ucsb.edu/online/dynamo_c08/cattaneo)
- F. Cattaneo, S.I. Vainshtein, Suppression of turbulent transport by a weak magnetic field. *Astrophys. J. Lett.* **376**, L21–L24 (1991)
- F. Cattaneo, N.H. Brummell, K.S. Cline, What is a flux tube? On the magnetic field topology of buoyant flux structures. *Mon. Not. R. Astron. Soc.* **365**, 727–734 (2006)
- S. Childress, Alpha-effect in flux ropes and sheets. *Phys. Earth Planet. Int.* **20**, 172–180 (1979)
- K.S. Cline, N.H. Brummell, F. Cattaneo, On the formation of magnetic structures by the combined action of velocity shear and magnetic buoyancy. *Astrophys. J.* **588**, 630–644 (2003a)
- K.S. Cline, N.H. Brummell, F. Cattaneo, Dynamo action driven by shear and magnetic buoyancy. *Astrophys. J.* **599**, 1449–1468 (2003b)
- A. Courvoisier, D.W. Hughes, S.M. Tobias, α -effect in a family of chaotic flows. *Phys. Rev. Lett.* **96**, 034503 (2006)
- T.G. Cowling, The magnetic field of sunspots. *Mon. Not. R. Astron. Soc.* **94**, 39–48 (1933)
- E.E. DeLuca, P.A. Gilman, Dynamo theory for the interface between the convection zone and the radiative interior of a star. Part I. Model Equations and exact solutions. *Geophys. Astrophys. Fluid Dyn.* **37**, 85–127 (1986)
- E.E. DeLuca, P.A. Gilman, Dynamo theory for the interface between the convection zone and the radiative interior of a star. Part II. Numerical solutions of the nonlinear equations. *Geophys. Astrophys. Fluid Dyn.* **43**, 119–148 (1988)
- M. Dikpati, P. Charbonneau, A Babcock-Leighton flux transport dynamo with solar-like differential rotation. *Astrophys. J.* **518**, 508–520 (1999)
- M. Dikpati, P. Gilman, Flux transport solar dynamos. *Space Sci. Rev.* (2009, this issue)
- S. D’Silva, A.R. Choudhuri, A theoretical model for tilts of bipolar magnetic regions. *Astron. Astrophys.* **272**, 621–633 (1993)
- G.B. Field, E.G. Blackman, Dynamical quenching of the α^2 dynamo. *Astrophys. J.* **572**, 685–692 (2002)
- U. Frisch, A. Pouquet, J. Léorat, A. Mazure, Possibility of an inverse cascade of magnetic helicity in hydrodynamic turbulence. *J. Fluid Mech.* **68**, 769–778 (1975)

- A. Giesecke, U. Ziegler, G. Rüdiger, Geodynamo α -effect derived from box simulations of rotating magnetoconvection. *Phys. Earth Planet. Int.* **152**, 90–102 (2005)
- A.V. Gruzinov, P.H. Diamond, Self-consistent theory of mean-field electrodynamics. *Phys. Rev. Lett.* **72**, 1651–1653 (1994)
- A.V. Gruzinov, P.H. Diamond, Self-consistent mean field electrodynamics of turbulent dynamos. *Phys. Plasmas* **2**, 1941–1947 (1995)
- A. Herzenberg, Geomagnetic dynamos. *Proc. R. Soc. Lond.* **250A**, 543–583 (1958)
- A. Hubbard, A. Brandenburg, Memory effects in turbulent transport, *Astrophys. J.* (2008). [arXiv:0811.2561](https://arxiv.org/abs/0811.2561)
- D.W. Hughes, M.R.E. Proctor, Large-scale dynamo action driven by velocity shear and rotating convection. *Phys. Rev. Lett.* **102**, 044501 (2009)
- A.B. Iskakov, A.A. Schekochihin, S.C. Cowley, J.C. McWilliams, M.R.E. Proctor, Numerical demonstration of fluctuation dynamo at low magnetic Prandtl numbers. *Phys. Rev. Lett.* **98**, 208501 (2007)
- P.J. Käpylä, A. Brandenburg, Turbulent dynamos with shear and fractional helicity. *Astrophys. J.* (2008, submitted). [arXiv:0810.2298](https://arxiv.org/abs/0810.2298)
- P.J. Käpylä, M.J. Korpi, A. Brandenburg, Large-scale dynamos in turbulent convection with shear. *Astron. Astrophys.* **491**, 353–362 (2008a)
- P.J. Käpylä, M.J. Korpi, A. Brandenburg, Alpha effect and turbulent diffusion from convection. *Astron. Astrophys.* (2008b). [arXiv:0812.1792](https://arxiv.org/abs/0812.1792)
- P.J. Käpylä, M.J. Korpi, A. Brandenburg, Large-scale dynamos in rigidly rotating turbulent convection. *Astrophys. J.* (2008c). [arXiv:0812.3958](https://arxiv.org/abs/0812.3958)
- L.L. Kitchatinov, M.V. Mazur, Stability and equilibrium of emerged magnetic flux. *Sol. Phys.* **191**, 325–340 (2000)
- N. Kleorin, I. Rogachevskii, Effective Ampère force in developed magnetohydrodynamic turbulence. *Phys. Rev.* **50**, 2716–2730 (1994)
- N. Kleorin, D. Moss, I. Rogachevskii, D. Sokoloff, Helicity balance and steady-state strength of the dynamo generated galactic magnetic field. *Astron. Astrophys.* **361**, L5–L8 (2000)
- E. Knobloch, Turbulent diffusion of magnetic fields. *Astrophys. J.* **225**, 1050–1057 (1978)
- F. Krause, The cosmic dynamo: from $t = -\infty$ to Cowling's theorem. A review on history, in *The Cosmic Dynamo*, ed. by F. Krause, K.-H. Rädler, G. Rüdiger (Kluwer, Dordrecht, 1993), pp. 487–499
- J. Larmor, How could a rotating body such as the Sun become a magnet. *Rep. Brit. Assoc. Adv. Sci.* **159** (1919)
- J. Larmor, The magnetic field of sunspots. *Mon. Not. R. Astron. Soc.* **94**, 469–471 (1934)
- D. Layzer, R. Rosner, H.T. Doyle, On the origin of solar magnetic fields. *Astrophys. J.* **229**, 1126–1137 (1979)
- F.J. Lowes, I. Wilkinson, Geomagnetic dynamo: a laboratory model. *Nature* **198**, 1158–1160 (1963)
- F.J. Lowes, I. Wilkinson, Geomagnetic dynamo: an improved laboratory model. *Nature* **219**, 717–718 (1968)
- J. Maron, E.G. Blackman, Effect of fractional kinetic helicity on turbulent magnetic dynamo spectra. *Astrophys. J. Lett.* **566**, L41–L44 (2002)
- P.D. Mininni, Y. Ponty, D.C. Montgomery, J.-F. Pinton, H. Politano, A. Pouquet, Dynamo regimes with a nonhelical forcing. *Astrophys. J.* **853**, 853–863 (2005)
- D. Mitra, P.J. Käpylä, R. Tavakol, A. Brandenburg, Alpha effect and diffusivity in helical turbulence with shear. *Astron. Astrophys.* (2008a, in press). [arXiv:0806.1608](https://arxiv.org/abs/0806.1608)
- D. Mitra, R. Tavakol, A. Brandenburg, D. Moss, Turbulent dynamos in spherical shell segments of varying geometrical extent. *Astrophys. J.* (2008b, submitted). [arXiv:0812.3106](https://arxiv.org/abs/0812.3106)
- Å. Nordlund, A. Brandenburg, R.L. Jennings, M. Rieutord, J. Ruokolainen, R.F. Stein, I. Tuominen, Dynamo action in stratified convection with overshoot. *Astrophys. J.* **392**, 647–652 (1992)
- E.N. Parker, Hydromagnetic dynamo models. *Astrophys. J.* **122**, 293–314 (1955)
- E.N. Parker, A solar dynamo surface wave at the interface between convection and nonuniform rotation. *Astrophys. J.* **408**, 707–719 (1993)
- J.H. Piddington, Turbulent diffusion of magnetic fields in astrophysical plasmas. *Astrophys. J.* **247**, 293–299 (1981)
- Y. Ponty, H. Politano, J.-F. Pinton, Simulation of induction at low magnetic Prandtl number. *Phys. Rev. Lett.* **92**, 144503 (2004)
- Y. Ponty, P.D. Mininni, D.C. Montgomery, J.-F. Pinton, H. Politano, A. Pouquet, Numerical study of dynamo action at low magnetic Prandtl numbers. *Phys. Rev. Lett.* **94**, 164502 (2005)
- K.-H. Rädler, A. Brandenburg, Mean-field effects in the Galloway-Proctor flow. *Mon. Not. R. Astron. Soc.* **393**, 113–125 (2009)
- K.-H. Rädler, M. Rheinhardt, Mean-field electrodynamics: critical analysis of various analytical approaches to the mean electromotive force. *Geophys. Astrophys. Fluid Dyn.* **101**, 11–48 (2007)
- K.-H. Rädler, M. Rheinhardt, E. Apstein, H. Fuchs, On the mean-field theory of the Karlsruhe dynamo experiment. *Nonlinear Processes Geophys.* **38**, 171–187 (2002)

- G.O. Roberts, Dynamo action of fluid motions with two-dimensional periodicity. *Phil. Trans. R. Soc.* **A271**, 411–454 (1972)
- I. Rogachevskii, N. Kleorin, Electromotive force and large-scale magnetic dynamo in a turbulent flow with a mean shear. *Phys. Rev.* **68**, 036301 (2003)
- I. Rogachevskii, N. Kleorin, Nonlinear theory of a ‘shear–current’ effect and mean-field magnetic dynamos. *Phys. Rev.* **70**, 046310 (2004)
- G. Rüdiger, A. Brandenburg, A solar dynamo in the overshoot layer: cycle period and butterfly diagram. *Astron. Astrophys.* **296**, 557–566 (1995)
- G. Rüdiger, V.V. Pipin, Viscosity-alpha and dynamo-alpha for magnetically driven compressible turbulence in Kepler disks. *Astron. Astrophys.* **362**, 756–761 (2000)
- G. Rüdiger, V.V. Pipin, G. Belvédère, Alpha-effect, helicity and angular momentum transport for a magnetically driven turbulence in the solar convection zone. *Sol. Phys.* **198**, 241–251 (2001)
- A.A. Shekochihin, N.E.L. Haugen, A. Brandenburg, S.C. Cowley, J.L. Maron, J.C. McWilliams, Onset of small-scale dynamo at small magnetic Prandtl numbers. *Astrophys. J.* **625**, L115–L118 (2005)
- M. Schrunner, K.-H. Rädler, D. Schmitt, M. Rheinhardt, U. Christensen, Mean-field view on rotating magnetoconvection and a geodynamo model. *Astron. Nachr.* **326**, 245–249 (2005)
- M. Schrunner, K.-H. Rädler, D. Schmitt, M. Rheinhardt, U.R. Christensen, Mean-field concept and direct numerical simulations of rotating magnetoconvection and the geodynamo. *Geophys. Astrophys. Fluid Dyn.* **101**, 81–116 (2007)
- M. Schüssler, Is there a phase constraint for solar dynamo models? *Astron. Astrophys.* **439**, 749–750 (2005)
- E.A. Spiegel, N.O. Weiss, Magnetic activity and variation in the solar luminosity. *Nature* **287**, 616–617 (1980)
- M. Steenbeck, F. Krause, Zur Dynamotheorie stellarer und planetarer Magnetfelder I. Berechnung sonnenähnlicher Wechselfeldgeneratoren. *Astron. Nachr.* **291**, 49–84 (1969)
- M. Steenbeck, F. Krause, K.-H. Rädler, Berechnung der mittleren Lorentz-Feldstärke $\mathbf{v} \times \mathbf{B}$ für ein elektrisch leitendes Medium in turbulenter, durch Coriolis-Kräfte beeinflusster Bewegung. *Z. Naturforsch.* **21a**, 369–376 (1966). See also the translation in Roberts & Stix, The turbulent dynamo, Tech. Note 60, NCAR, Boulder, Colorado (1971)
- M. Stix, Differential rotation and the solar dynamo. *Astron. Astrophys.* **47**, 243–254 (1976)
- K. Subramanian, A. Brandenburg, Nonlinear current helicity fluxes in turbulent dynamos and alpha quenching. *Phys. Rev. Lett.* **93**, 205001 (2004)
- K. Subramanian, A. Brandenburg, Magnetic helicity density and its flux in weakly inhomogeneous turbulence. *Astrophys. J.* **648**, L71–L74 (2006)
- S. Sur, K. Subramanian, A. Brandenburg, Kinetic and magnetic alpha effects in nonlinear dynamo theory. *Mon. Not. R. Astron. Soc.* **376**, 1238–1250 (2007)
- S. Sur, A. Brandenburg, K. Subramanian, Kinematic alpha effect in isotropic turbulence simulations. *Mon. Not. R. Astron. Soc.* **385**, L15–L19 (2008)
- H. Svensmark, Imprint of Galactic dynamics on Earth’s climate. *Astron. Nachr.* **327**, 866–870 (2007a)
- H. Svensmark, Cosmic rays and the biosphere over 4 billion years. *Astron. Nachr.* **327**, 871–875 (2007b)
- J.-C. Thelen, A mean electromotive force induced by magnetic buoyancy instabilities. *Mon. Not. R. Astron. Soc.* **315**, 155–164 (2000)
- A. Tilgner, Magnetohydrodynamic flow in precessing spherical shells. *J. Fluid Mech.* **379**, 303–318 (1999)
- A. Tilgner, A. Brandenburg, A growing dynamo from a saturated Roberts flow dynamo. *Mon. Not. R. Astron. Soc.* **391**, 1477–1481 (2008)
- S. Tobias, Relating stellar cycle periods to dynamo calculations. *Mon. Not. R. Astron. Soc.* **296**, 653–661 (1998)
- S.M. Tobias, F. Cattaneo, N.H. Brummell, Convective dynamos with penetration, rotation, and shear. *Astrophys. J.* **685**, 596–605 (2008)
- S.I. Vainshtein, F. Cattaneo, Nonlinear restrictions on dynamo action. *Astrophys. J.* **393**, 165–171 (1992)
- E.T. Vishniac, J. Cho, Magnetic helicity conservation and astrophysical dynamos. *Astrophys. J.* **550**, 752–760 (2001)
- N.O. Weiss, Linear and nonlinear dynamos. *Astron. Nachr.* **326**, 157–165 (2005)
- H. Yoshimura, Phase relation between the poloidal and toroidal solar-cycle general magnetic fields and location of the origin of the surface magnetic fields. *Sol. Phys.* **50**, 3–23 (1976)
- T.A. Yousef, A. Brandenburg, G. Rüdiger, Turbulent magnetic Prandtl number and magnetic diffusivity quenching from simulations. *Astron. Astrophys.* **411**, 321–327 (2003)